

$^{144}\text{Sm}(^{16}\text{O},5\text{n}\gamma)$  2016Li41

Type	Author	History Citation	Literature Cutoff Date
Full Evaluation	N. Nica	NDS 160, 1 (2019)	21-Oct-2019

$E(^{16}\text{O})=118$  MeV beam provided by Separated Sector Cyclotron (SSC) at iThemba LABS, South Africa on  $2.89$  mg/cm<sup>2</sup> target (on  $13.13$  mg/cm<sup>2</sup> Pb backing). Used  $\gamma$  multidetector array AFRODITE (8 Compton-suppressed clover detectors). Energy and efficiency calibrations performed with standard  $^{133}\text{Ba}$  and  $^{152}\text{Eu}$  sources. Measured symmetrized  $\gamma\gamma$  and  $\gamma\gamma\gamma$  coin and asymmetric Angular Distribution from Oriented states (ADO)  $\gamma\gamma$  coin matrices. Specific reaction channels selection done with the so called chessboard comprising 24 CsI scintillators. Semiempirical shell-model (SESM) calculations. Coexistence of prolate-oblate shapes predicted by adiabatic and configuration-fixed constrained triaxial covariant density functional theory (CDFT) calculations with point-coupling energy density functional (PC-PK1). Also performed potential energy surfaces calculations and systematics of N=85 even-Z isotones, N=87 even-Z isotones, N=84 even-even isotones, and N=86 even-even isotones comparisons respectively.

 $^{155}\text{Yb}$  Levels

E(level) <sup>†</sup>	$J^{\pi\ddagger}$	$T_{1/2}$	Comments
0.0 <sup>#</sup>	(7/2 <sup>-</sup> )	1.793 s 19	$J^{\pi}, T_{1/2}$ : from the adopted values. configuration: ( $\nu f_{7/2}$ ) $7/2^{-}$ , oblate, $\beta=0.15$ , $\gamma\approx 60^{\circ}$ .
168.7 <sup>@</sup> 3	(9/2 <sup>-</sup> )		configuration: ( $\nu h_{9/2}$ ) $9/2^{-}$ , prolate, $\beta=0.14$ , $\gamma\approx 0^{\circ}$ .
666.00 <sup>#</sup> 19	(11/2 <sup>-</sup> )		
839.4 <sup>&amp;</sup> 3	(13/2 <sup>+</sup> )		configuration: ( $\nu i_{13/2}$ ) $13/2^{+}$ , oblate, $\beta=0.16$ , $\gamma\approx 60^{\circ}$ .
983.8 <sup>@</sup> 4	(13/2 <sup>-</sup> )		
1178.5 <sup>#</sup> 3	(15/2 <sup>-</sup> )		
1527.5 <sup>&amp;</sup> 3	(17/2 <sup>+</sup> )		
1592.8 <sup>@</sup> 4	(17/2 <sup>-</sup> )		
1912.8 <sup>@</sup> 5	(21/2 <sup>-</sup> )		
2033.7 <sup>&amp;</sup> 5	(21/2 <sup>+</sup> )		
2494.4 <sup>&amp;</sup> 6	(25/2 <sup>+</sup> )		
2526.6 6	(23/2 <sup>-</sup> )		
2768.8 <sup>@</sup> 6	(25/2 <sup>-</sup> )		
3520.3 <sup>@</sup> 8	(29/2 <sup>-</sup> )		
3740.8 <sup>@</sup> 9	(33/2 <sup>-</sup> )		
4183.4 11	(35/2 <sup>-</sup> )		
4549.6 12	(37/2 <sup>-</sup> )		

<sup>†</sup> From least-squares fit to  $E\gamma$ 's.

<sup>‡</sup> Values assigned by 2016Li41 based on measured multiplicities, systematics and theoretical calculations.

<sup>#</sup> Band(A): Based on ( $\nu f_{7/2}$ ) $7/2^{-}$ . Levels (7/2<sup>-</sup>), (11/2<sup>-</sup>), (15/2<sup>-</sup>) proposed to arise from the coupling of the  $\nu f_{7/2}$  orbital to the 0<sup>+</sup>, 2<sup>+</sup>, 4<sup>+</sup> couplings of the two  $\nu f_{7/2}$  orbitals (2016Li41).

<sup>@</sup> Band(B): Based on ( $\nu h_{9/2}$ ) $9/2^{-}$ . Levels (9/2<sup>-</sup>), (13/2<sup>-</sup>), (17/2<sup>-</sup>), (21/2<sup>-</sup>) proposed to arise from the coupling of the  $\nu h_{9/2}$  orbital to the 0<sup>+</sup>, 2<sup>+</sup>, 4<sup>+</sup>, 6<sup>+</sup> couplings of the two  $\nu f_{7/2}$  orbitals (2016Li41).

<sup>&</sup> Band(C): Based on ( $\nu i_{13/2}$ ) $13/2^{+}$ . Levels (13/2<sup>+</sup>), (17/2<sup>+</sup>), (21/2<sup>+</sup>), (25/2<sup>+</sup>) proposed to arise from the coupling of the  $\nu i_{13/2}$  orbital to the 0<sup>+</sup>, 2<sup>+</sup>, 4<sup>+</sup>, 6<sup>+</sup> couplings of the two  $\nu f_{7/2}$  orbitals (2016Li41).

$^{144}\text{Sm}(^{16}\text{O},5n\gamma)$  **2016Li41** (continued)

$\gamma(^{155}\text{Yb})$							
$E_\gamma$ †	$I_\gamma$ ‡	$E_i(\text{level})$	$J_i^\pi$	$E_f$	$J_f^\pi$	Mult. @	Comments
168.7 4	37.7 6	168.7	(9/2 <sup>-</sup> )	0.0	(7/2 <sup>-</sup> )	(M1+E2)	ADO=0.97 2.
173.4 2	98.2 <sup>#</sup> 54	839.4	(13/2 <sup>+</sup> )	666.00	(11/2 <sup>-</sup> )	D(+Q)	ADO=0.75 1.
220.5 5	32.5 6	3740.8	(33/2 <sup>-</sup> )	3520.3	(29/2 <sup>-</sup> )	E2	ADO=1.29 2.
242.2 5	16.6 3	2768.8	(25/2 <sup>-</sup> )	2526.6	(23/2 <sup>-</sup> )	(M1+E2)	ADO=0.95 2.
317.8 5		983.8	(13/2 <sup>-</sup> )	666.00	(11/2 <sup>-</sup> )		
320.0 3	70.3 6	1912.8	(21/2 <sup>-</sup> )	1592.8	(17/2 <sup>-</sup> )	E2	ADO=1.38 2.
349.0 3	71.5 <sup>#</sup> 25	1527.5	(17/2 <sup>+</sup> )	1178.5	(15/2 <sup>-</sup> )	D(+Q)	ADO=0.86 2.
366.2 5	15.9 2	4549.6	(37/2 <sup>-</sup> )	4183.4	(35/2 <sup>-</sup> )	D	ADO=0.79 1.
414.3 5		1592.8	(17/2 <sup>-</sup> )	1178.5	(15/2 <sup>-</sup> )		
442.6 5	20.8 4	4183.4	(35/2 <sup>-</sup> )	3740.8	(33/2 <sup>-</sup> )	(M1+E2)	ADO=0.68 2.
460.7 3	68.3 <sup>#</sup> 28	2494.4	(25/2 <sup>+</sup> )	2033.7	(21/2 <sup>+</sup> )	E2	ADO=1.36 7.
506.2 3	70.0 <sup>#</sup> 10	2033.7	(21/2 <sup>+</sup> )	1527.5	(17/2 <sup>+</sup> )		ADO=1.07 3.
							Mult.: based on ADO ratio this should be D+Q; <b>2016Li41</b> adopt Q as in band transition.
512.5 3	75.4 <sup>#</sup> 26	1178.5	(15/2 <sup>-</sup> )	666.00	(11/2 <sup>-</sup> )		
609.0 2	80.2 14	1592.8	(17/2 <sup>-</sup> )	983.8	(13/2 <sup>-</sup> )	E2	ADO=1.29 3.
613.8 5	18.3 7	2526.6	(23/2 <sup>-</sup> )	1912.8	(21/2 <sup>-</sup> )	(M1+E2)	ADO=0.67 2.
666.0 2	178.8 <sup>#</sup> 54	666.00	(11/2 <sup>-</sup> )	0.0	(7/2 <sup>-</sup> )	E2	ADO=1.28 3.
688.1 2	100 <sup>#</sup>	1527.5	(17/2 <sup>+</sup> )	839.4	(13/2 <sup>+</sup> )	E2	ADO=1.24 7.
751.5 5	35.2 7	3520.3	(29/2 <sup>-</sup> )	2768.8	(25/2 <sup>-</sup> )	E2	ADO=1.30 3.
815.1 2	100	983.8	(13/2 <sup>-</sup> )	168.7	(9/2 <sup>-</sup> )	E2	ADO=1.35 3.
856.0 4	46.3 5	2768.8	(25/2 <sup>-</sup> )	1912.8	(21/2 <sup>-</sup> )		ADO=1.01 2.
							Mult.: based on ADO ratio this should be D+Q; <b>2016Li41</b> adopt Q as in band transition.

† Based on comment of **2016Li41** that uncertainties are between 0.2 and 0.5 keV the evaluator assigned unc to each  $\gamma$  transition based on their relative intensities divided into four groups covering the interval in between 16%–100% starting with 0.5 keV for the lowest intensity group up to 0.2 keV for the highest one ending to 100%, here including the 179% higher relative intensity. No difference was made in between the two groups based on the two different normalizations (see the comment below).

‡ **2016Li41** give two scales of normalization  $\gamma$ -ray intensities: normalized to 100% for 815.1 $\gamma$  unless noted otherwise.

# Normalized to 100% for 688.1 $\gamma$ .

@ From measured experimental ratio  $R_{\text{ADO}}=I_\gamma(135^\circ)/I_\gamma(90^\circ)$  with typical values 1.2 for stretched quadrupole and 0.8 for stretched pure dipole transitions respectively. For the particular population and decay mechanism of this study **2016Li41** adopted E2 for stretched Q (M2 is unlikely) and (M1+E2) for mixed D+Q transitions (E1+M2 is less likely) while for the relatively pure dipole transitions one can rather adopt D(+Q).

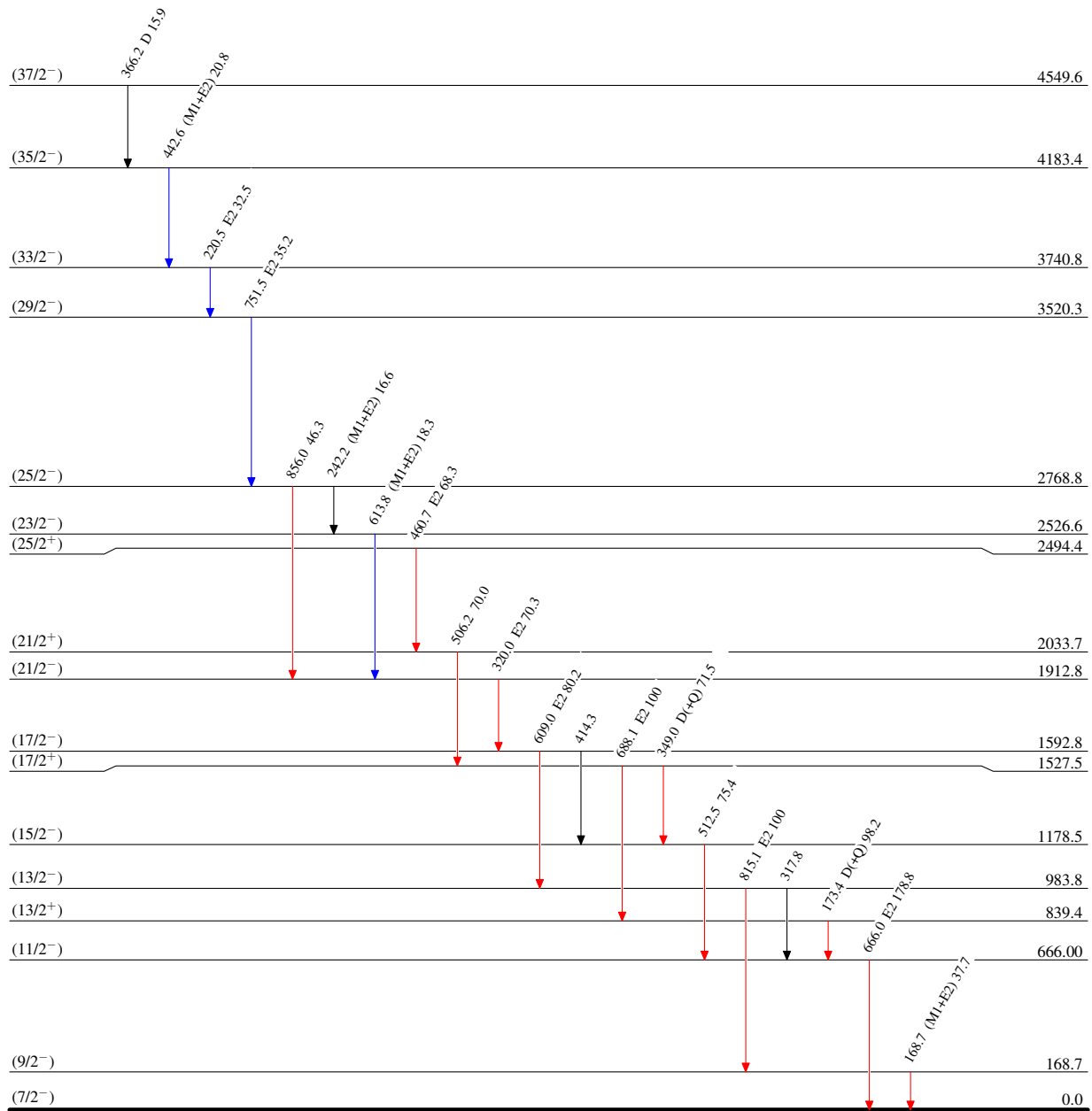
$^{144}\text{Sm}(^{16}\text{O},5n\gamma)$  2016Li41

## Level Scheme

Intensities: Relative  $I_\gamma$ 

## Legend

- $I_\gamma < 2\% \times I_\gamma^{\text{max}}$
- $I_\gamma < 10\% \times I_\gamma^{\text{max}}$
- $I_\gamma > 10\% \times I_\gamma^{\text{max}}$



1.793 s 19

 $^{155}_{70}\text{Yb}_{85}$

$^{144}\text{Sm}(^{16}\text{O},5n\gamma) \quad 2016\text{Li41}$ 